Sensors & Transducers, Vol. 260, Issue 1, May 2023, pp. 1-6

Sensors & Transducers
Published by IFSA Publishing, S. L., 2023
http://www.sensorsportal.com

Rapid Evaluation of Mandarin Crop Water Stress Index using CWSI Infrared Camera

[1,*] Sadick Amoakohene APPIAH, [1] Jiuhao LI, [1] Kelvin Edom ALORDZINU, [2] Fuseini ISSAKA, [3] Ebenezer Acheampong AFFUL, [4] Evans ASENSO, [5] Ransford Opoku DARKO, [1] Alaa AL AASMI and [1] Qiao SONGYANG

[1] College of Water Conservancy and Civil Engineering, South China Agricultural University, No. 483, Wushan Road, Tianhe District, Guangzhou 510642, China
[2] P.M.B Academy Post Office, Soil, Water and Environmental Engineering Division, Soil Research Institute of Ghana, Kumasi, Ghana
[3] Soil Science Division, Cocoa Research Institute of Ghana (Ghana COCOBOD), New Tafo-Akim, Ghana
[4] Department of Agricultural Engineering, University of Ghana, Accra, Ghana
[5] Department of Agricultural Engineering, University of Cape Coast, Cape Coast, Ghana
E-mail: aasadick07@ gmail.com, jhli@scau.edu.cn, kelvinedomalordzinu@stu.scau.edu.cn, alaaasmi83@gmail.com, qsy1999@stu.scau.edu.cn, fuseini-issaka@csir.org.gh, ebenezer.afful@crig.org.gh easenso@ug.edu.gh, ransford.darko@ucc.edu.gh

Received:27 March 2023 /Accepted: 30 April 2023/ Published: 23 May 2023

Abstract: The "Workswell Wiris Agro R Infrared camera" (WWARIC) was utilized to monitor and detect water stress conditions in mandarin, as well as predicting optimal irrigation regimes. Air temperature, canopy temperature, and vapor pressure deficits were similarly measured and subsequently used to compute crop water stress index empirically using Idso techniques ($CWSI_{Idso}$). Baseline equations were established for transpiring and non-transpiring conditions in mandarin. $CWSI_{Idso}$ and CWSI calculated from the WWARIC ($CWSI_W$) depicted a high correlation ($R^2 = 0.75$ at $p< 0.05$) in measuring the level of water stress in mandarin. The WWARIC was also able to detect water stress in all three camera modes (empirical, differential and theoretical) at a height of 12 meters above the mandarin canopy. The results showed that the WWARIC could effectively identify mandarin water stress with enough precision, speed, and in real time showing water stress in different ranges and colors.

Keywords: Infrared thermometry, Crop water stress index, Baseline equations, Real-time, Workswell Wiris Agro R infrared camera.

1. Introduction

Climate change, urban sprawl, rapid industrialization, high population growth, and rising demand for fresh water for domestic and commercial purposes are all major threats to irrigated agriculture globally [1,2]. When left unchecked, this condition will result in crop production under limited water availability (water-stressed conditions), with the ensuing output being deleterious [3,4].

The most widely used approaches in monitoring water stress in tree crops (water potentials and stomatal conductance gs) are demanding, time consuming, cannot be easily automated, and only give a point measurement in a leaf, a single soil location, branch, or tree [5, 6]. Additionally, the reliability of data obtained from water potential (Ψ) measurements may be low because water potential (Ψ) reduces in isohydric plant species (example mandarin) since effective stomatal regulation can be preserved by these species. This feature hinders noticeable decrease in water potential (Ψ) during limiting water (drought) conditions or during periods of high evaporative demand [6].

The use of infrared thermometry and its associated devices from space to investigate the fluctuations in plant canopy temperature as the state of plant water changes has been successful [5, 7]. In commercial orchards, less sophisticated and automated remote sensing technologies are important to rapidly and precisely estimate plant-water status in order to minimize yield reduction and production losses resulting from water deficit [5, 8, 9].

The Crop water stress index (CWSI) has been normalized to assess the extent of crop water stress while curtailing the effects of ecological conditions influencing the interactions between air temperature and plant canopy temperature [7, 10, 11]. Measurement of CWSI is developed on the relationship connecting actual canopy temperature (Tc) vis a vis the theoretical canopy temperature data obtained from two different thresholds namely; a lower limit (when maximum plant transpiration is achieved under full irrigation when stomata are completely opened) and an upper limit (when plants are not transpiring because they are under extreme water stress conditions leading to complete stomata closure) [5, 10, 12].

Currently, the CWSI model is used to detect water status in most crops. However, the technicalities, tedious and arduous procedures used during the computations of CWSI values in assessing plant water stress result in low farmer-researcher adaptability [5, 12, 13]. To minimize the problems of farmer-researcher compliance and other related issues, the CWSI camera has been designed to effectively evaluate crop water stress promptly independent of secondary weather data, complex mathematical and scientific formulae and workable operating system software.

The aim of this experiment is to study the efficiency and possibility of using the "WWARIC" to monitor water stress and to appropriately schedule irrigation regimes in mandarin.

2 Materials and Methods

2.1. Experimental Site and Design

A four-by-three randomized complete block design (RCBD) was used for the experiment at the South China Agricultural University Citrus Experimental Orchard near Yangcun town. 36 mandarin pants were subjected to 4 water treatment levels; full irrigation (80–100 % FC) and regulated deficit irrigation schedules (70–75 % FC, 60–65 % FC and 50–55 % FC).

Water was supplied using a gravity-driven drip system with an adjusted flow rate of 6 L/h. Before each irrigation scheduling, the soil gravimetric water content was measured and expressed in terms of volumetric water content (θv). These data were compared with the soil water content (θv) data obtained by measuring with an IMKO TRIMETDR probe that was inserted horizontally along the walls of ditches dug closed to the plant root zone (about 0.5 m from the base of the plant) at different depth intervals. The amount of irrigation water applied was estimated from the equation used by [14, 15] as

$$d_n = \left(\left(\frac{FC - SMC}{100}\right) \times BD \times D\right), \qquad (1)$$

where FC is the field capacity of the soil, BD is the bulk density of the soil, D is the rootzone depth, SMC is the prevailing soil moisture content on a volume basis, and dn = amount of irrigation water applied.

2.2. Estimating CWSI and Relative Leaf Water Content

Weekly CWSI using Idso approach and Relative Leaf Water Content were determined from the equations (1) and (2) respectively

$$\mathrm{CWSI}_{(\mathrm{Idso})=\frac{(\mathrm{T}_c - \mathrm{T}_a) - \mathrm{D}_2}{\mathrm{D}_1 - \mathrm{D}_2}} \qquad (2)$$

where T_c is the mandarin leaf cover temperature (°C); T_a is the orchard air temperature (°C); D_2 is the lower reference point and D_1 = the upper reference point.

$$\mathrm{RLWC} = \frac{(\mathrm{FW} - \mathrm{DW})}{(\mathrm{TW} - \mathrm{DW})} \times 100, \qquad (3)$$

where RLWC (%) = the relative leaf water content, FW = the weight of fresh leaves, DW = the weight of dried leaves, and TW = the weight of turgid leaves.

2.3. Estimating CWSI using the WWARIC

The Workswell Wiris Agro R infrared camera has an inbuilt four-color map with full radiometric (temperature) information. The camera can be operated rapidly to capture videos and images simultaneously as thermal imagery, digital imagery, or digital video imagery. During operation, the camera images can be viewed as picture-in-picture (PIP), full screen RGB with segmentation, or dual-screen. There are three micro-HDMI video outputs in the formats: 1280 × 720 pixels (720p), an aspect ratio of 16:9, and a micro-HDMI video output.

Aerial images captured with the WWARIC were processed with CorePlayer software version 1.4.1. The $CWSI_W$ was compared with the $CWSI_{(Idso)}$ and the relative leaf water content (RLWC) to determine precision through correlation.

2.4. Data Analysis

Statistical analyses were conducted using the IBM SPSS version 21 software. One-way ANOVA was used to analyze the differences in the water stress parameters studied (the leaf temperature (LT°C), the relative leaf water content (RLWC) (%), the leaf chlorophyll content (LCC) (mg g^{-1}), and the water stress index, $CWSI_{(Idso)}$) within treatments and blocks. The treatment means were separated by the Tukey HSD method to indicate significant differences among the treatment means, at 0.001, 0.01, and 0.05 levels of significance.

3. Resuts

3.1. Empirical CWSI using Idso Approach and Baseline Equations

VPD and canopy-air temperature differences measured were significantly different (at $p < 0.001$) among treatments and within treatments, however, both parameters were strongly correlated to the CWSI determined from Idso procedures at $R^2 = 0.67$ and $R^2 = 0.79$ respectively as seen in Fig. 1.

The estimated CWSI(Idso) values ranged from −0.21 to 0.79, with average values of 0.15, 0.33, 0.47, and 0.60 recorded for treatments 80–100 % FC, 70–75 % FC, 60–65 % FC, and 50–55 % FC, respectively. Graph of the estimated CWSI during the experimet is shown in Fig. 2.

The baseline equations developed for the mandarins were $\mathrm{Tc} - \mathrm{Ta} = -0.56 \times (\mathrm{VPD}) + 4.05$ for the transpiring baseline and $\mathrm{Tc} - \mathrm{Ta} = 4.05$ for non-transpiring baseline.

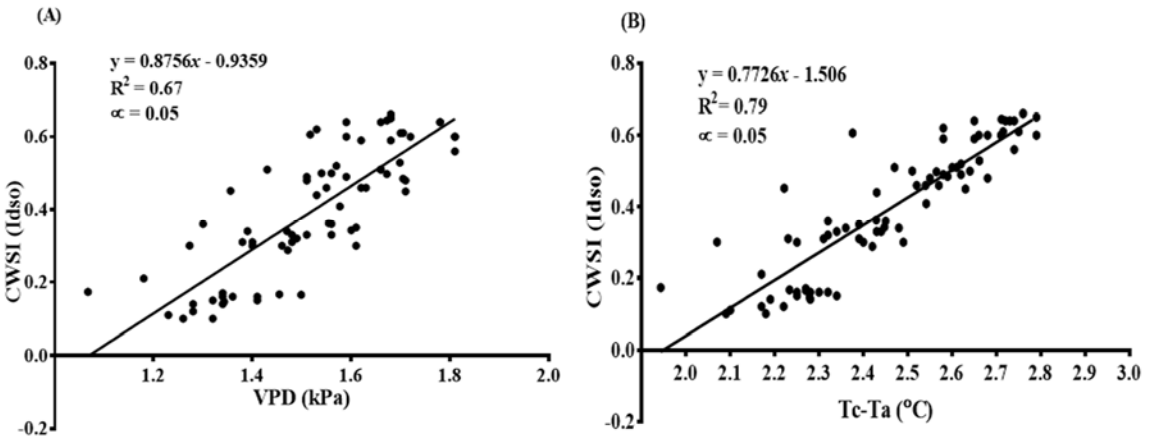

Fig. 1. Correlation between A. $CWSI_{(Idso)}$ and VPD (kPa) B. $CWSI_{(Idso)}$ and Tc-Ta (°C).

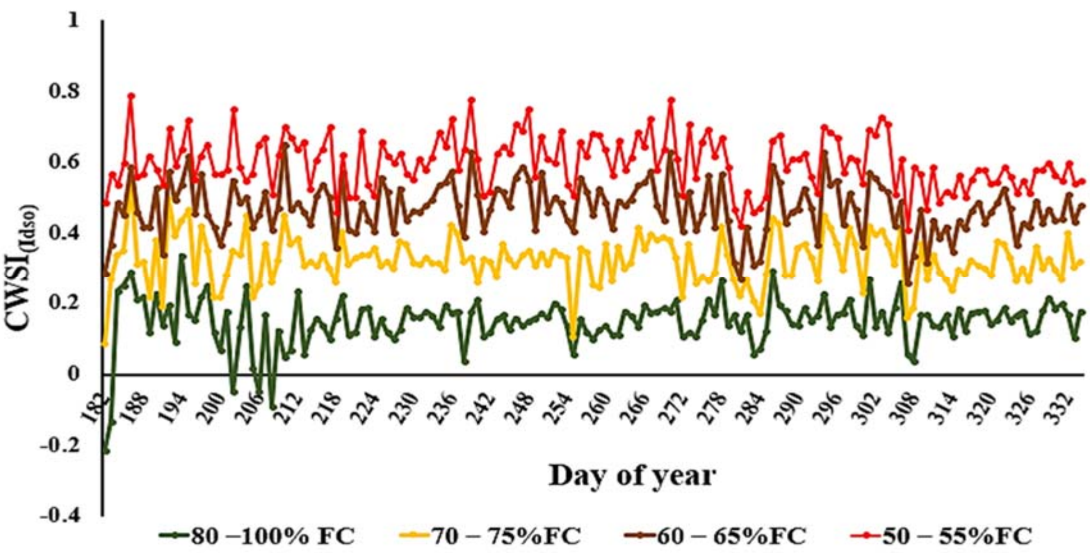

Fig. 2. Estimated $CWSI_{(Idso)}$.

3.2 Relative Leaf Water Content

The RLWC increased with increasing water available to the plant. RLWC increased steadily across all the treatments during the experiment, however, there were few weeks where there was little reduction in the values collected. The estimated average RLWC (%) estimated during the experiment was 93.93, 86.79, 84.59, and 82.88 for treatments 80–100 % FC, 70–75 % FC, 60–65 % FC, and 50–55% FC, respectively. The observed relative leaf water content for the study period is presented in Fig. 3.

3.3. Mandarin CWSI Estimated from the Workswell WIRIS Agro R Infrared Camera

Fig. 4 shows a digital image of the mandarin orchard captured using the WWARIC and the isothermal imagery obtained after processing with the WIRIS core player version 1.4.1 during a sample data collection session.

4. Discussion

The results revealed that, the CWSI computed using Idso approach increased with increasing soil water deficit. The average estimated CWSI from Idso approach for the period of study was in the order 80 – 100 % FC < 70 – 75 % FC < 60 – 65 % FC < 50 – 55 % FC which corresponded to CWSI values of 0.15 < 0.33 < 0.47 < 0.60. This is similar to the results of [12, 16–19] who observed that the CWSI in plants increases with decreasing water availability of in the soil and vise versa.

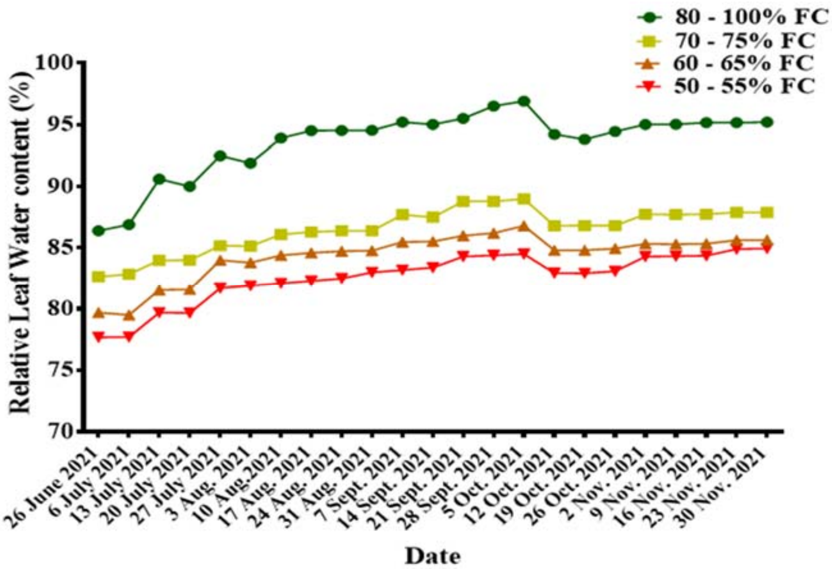

Fig. 3. Estimated RLWC (%).

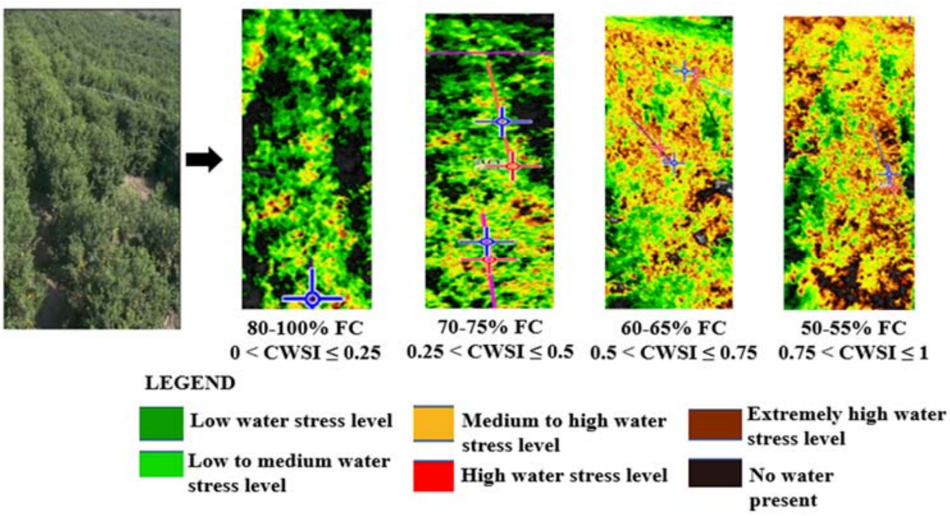

Fig. 4. Digital image and processed isothermal image.

The results of the estimated CWSI from the WWARIC on the four water application levels were established by categorizing the CWSI values into a 0.25 interval range comparable to the procedures proposed by [11,18,20]. The CWSI recorded during the measurement session under the 80 – 100% FC treatment were within the CWSI range of $0.00 < CWSI_W \leq 0.25$, which is shown by a deep green coloration, while treatments under 70 – 75 % FC water stress level were within the range $0.25 < CWSI_W \leq 0.5$ represented with a light green color. Also, CWSI for mandarin under 60 – 65% FC water stress level were within the $0.5 < CWSI_W \leq 0.75$ range which is represented by a yellow color while CWSI for mandarin under 50 – 55% FC water stress level were within the range $0.75 < CWSI_W \leq 1.00$ which is represented with light brown coloration. Nevertheless, CWSI value > 1 is indicated with dark brown color on the tiff image shows lack of (typically showing the mulch cover but not necessarily water stress within the canopy).

Moreover, the estimated CWSI from the field data was strongly correlated with the CWSI gained by the WWARIC ($R^2 = 0.75$) which indicates that the camera is capable of estimating the extent of stress a particular plant is subjected to in-situ and in real time in any plant condition. This outcome is similar to the results from [11], where the WWARIC was used to successfully study water stress in tomato grown under greenhouse conditions.

5. Conclusions

This novel WWARIC has demonstrated enough precision, swiftness, and intelligibility in the in-situ estimation of water stress in mandarin, presenting estimated CWSI in specific color ranges and values. The following colour codes were established from the studies; deep green colour represents plants under the treatment 80 – 100 % FC (little or no stress) within a range of $0 < \mathrm{CWSI} \leq 0.25$, light green colour indicates plants subjected to 70 – 75 % FC (mild to medium water stress level) for the range $0.25 < \mathrm{CWSI} \leq 0.5$, yellow colour represents plants under 60 – 65 % FC (medium to high water stress level) within the range $0.5 < \mathrm{CWSI} \leq 0.75$ and light brown colour depicts plants subjected to 50 – 55 % FC (high to extremely high water stress status) for the range $0.75 < \mathrm{CWSI} \leq 1$. However, the dark brown colours seen on the Tiff image represent complete drought or no water present ($\mathrm{CWSI} > 1$) which in this case was the image for the ground plastic mulch cover since there wasn't total drought situation during the study period. When adopted and used in precision agriculture, this camera will save significant time, money, and other resources.

Acknowledgments

We would like to acknowledge the efforts of everyone who contributed to the success of this article, especially the funding institution, the field workers, and the laboratory crew.

References

[1]. Al-Ghobari, H. M., Dewidar, A. Z. Integrating deficit irrigation into surface and subsurface drip irrigation as a strategy to save water in arid regions, *Agricultural Water Management,* 209, 2018, pp. 55-61.

[2]. Radmehr, A., Bozorg-Haddad, O., Loáiciga, H. A., Integrated strategic planning and multi-criteria decision-making framework with its application to agricultural water management, *Scientific Report,* 12, 2022, 8406.

[3]. Blanco, V., Blaya-Ros, P. J., Torres-Sánchez, R., Domingo, R. Influence of Regulated Deficit Irrigation and Environmental Conditions on Reproductive Response of Sweet Cherry Trees, *Plants,* 9, 2020, pp. 1–17.

[4]. Faghih, S., Zamani, Z., Fatahi, R., Liaghat, A., Effects of deficit irrigation and kaolin application on vegetative growth and fruit traits of two early ripening apple cultivars, *Biological Research,* 52, 2019, 43.

[5]. Romero-Trigueros, C., Gambín, J. M. B., Tortosa, P. A. N., Cabañero, J. J. A., Nicolás, E. N., Determination of Crop Water Stress Index by Infrared Thermometry in Grapefruit Trees Irrigated with Saline Reclaimed Water Combined with Deficit Irrigation, *Remote Sensing,* 11, 2019, pp. 3–20.

[6]. Ihuoma, S. O., The use of spectral reflectance data to assess plant stress and improve irrigation water management, *McGill University*, Montreal, 2020.

[7]. Drechsler, K., Kisekka, I., Upadhyaya, S., A comprehensive stress indicator for evaluating plant water status in almond trees, *Agricultural Water Management,* 216, 2019, pp. 214–223.

[8]. Ballester, C., Zarco-Tejada, P. J., Nicolás, E., Alarcón, J. J., Fereres, E., Intrigliolo, D. S., Gonzalez-Dugo, V., Evaluating the performance of xanthophyll, chlorophyll and structure-sensitive spectral indices to detect water stress in five fruit tree species, *Precision Agriculture,* 19, 2018, pp. 178–193.

[9]. Romero-Trigueros, C., Nortes, P. A., Alarcón, J. J., Hunink, J. E., Parra, M., Contreras, S., Droogers, P., Nicolás, E., Effects of saline reclaimed waters and deficit irrigation on Citrus physiology assessed by UAV remote sensing, *Agricultural Water Management,* Vol. 183, 2017, pp. 60-69.

[10]. Ru, C., Hu, X., Wang, W., Ran, H., Song, T., Guo, Y., Evaluation of the crop water stress index as an indicator for the diagnosis of grapevine water deficiency in greenhouses, *Horticulturae,* 6, 2020, pp. 1–19.

[11]. Alordzinu, K. E., Li, J., Lan, Y., Appiah, S. A., AL Aasmi, A., Wang, H., Rapid Estimation of Crop Water Stress Index on Tomato Growth, *Sensors,* 21, 2021, 5142.

[12]. Jackson, R. D., Idso, S. B., Reginato, R. J., Pinter, P. J., Canopy temperature as a crop water stress indicator. *Water Resources,* 17, 1981, pp. 1133–1138.

[13]. Idso, S. B., Jackson, R. D., Pinter, P. J., Hatfield, J. H., Normalizing the stress degree-day parameter for environmental variability, *Agricultural Meteorology,* 24, 1981, pp. 45–55.

[14]. Fahad, M., Wajid, S. A., Ahmad, A., Cheema, M. J. M., Response of wheat cultivars to deficit irrigation under semiarid conditions of Faisalabad, *International*

Journal of Agriculture and Biology, 21, 2019, pp. 1004–1012.

[15]. Khan, S., Rasool, A., Irshad, S., Hafeez, M.B., Ali, M., Saddique, M., Asif, M., Hasnain, Z., Naseem, S., Alwahibi, M.S., et al., Potential soil moisture deficit: A useful approach to save water with enhanced growth and productivity of wheat crop, *Journal of Water and Climate Change,* 12, 6, 2021, pp. 2515–2525.

[16]. Sepaskhah, A. R., Kashefipour, S. M., Evapotranspiration and crop coefficient of sweet lime under drip irrigation, *Agricultural Water Management,* 27, 1995, pp. 331–340.

[17]. Tanriverdi, C., Atilgan, A., Degirmenci, H., Akyuz, A., Comparison of Crop Water Stress Index (CWSI) and Water Deficit Index (WDI) by using Remote Sensing (RS), *Infrastructure and Ecology of Rural Areas,* 2017, pp. 879–894.

[18]. Veysi, S., Ali Naseri, A.B.D., Hamzeh, S., H Bartholomeus A satellite based crop water stress index for irrigation scheduling in sugarcane fields. *Agricultural Water Management,* 189, 2017, pp. 70–86.

[19]. DeJonge, K. C., Taghvaeian, S., Trout, T. J., Comas, L. H., Comparison of canopy temperature-based water stress indices for maize, *Agricultural Water Management,* 156, 2015, pp. 51–62.

[20]. Magney, T. S., Vierling, L. A., Eitel, J. U., Huggins, D. R., Garrity, S. R., Response of high frequency Photochemical Reflectance Index (PRI) measurements to environmental conditions in wheat, *Remote Sensing and Environment,* 173, 2016, pp. 84–97.

[21]. Appiah, S. A., Li, J., Alordzinu, K. E., Issaka, F., Afful, E. A., Asenso, E., Darko, R. O., Al Aasmi, A., Qiao, S., In-situ Assessment of Mandarin Crop Water Stress Index Using CWSI Infrared Camera, in *Proceedings of the 8th International Conference on Sensors and Electronic Instrumentation Advances*, 21-23 September 2022, Corfu Holiday Palace, Corfu, Greece, pp. 60-64.
